

$InBO_3$ Photocatalyst with Calcite Structure for Overall Water Splitting

Qingxin Jia,[1] Yugo Miseki,[1] Kenji Saito,[1] Hisayoshi Kobayashi,[2] and Akihiko Kudo*[1]

[1]Department of Applied Chemistry, Faculty of Science, Tokyo University of Science, 1-3 Kagurazaka, Shinjuku-ku, Tokyo 162-8601

[2]Department of Chemistry and Materials Technology, Kyoto Institute of Technology, Matsugasaki, Sakyo-ku, Kyoto 606-8585

Received May 10, 2010; E-mail: a-kudo@rs.kagu.tus.ac.jp

Indium borate ($InBO_3$) with a calcite structure that was prepared by a solid-state reaction and a two-step precipitation method was employed as a photocatalyst for water splitting under UV light irradiation. The $InBO_3$ photocatalyst prepared by the precipitation method showed higher activity than that prepared by the solid-state reaction when a NiO cocatalyst was loaded on the photocatalyst. In the case of the precipitation method, the photocatalytic activity over $NiO/InBO_3$ strongly depended on the calcination temperature and an excess amount of boric acid in the preparation. The correlation among preparation conditions, physical properties, and photocatalytic activities for water splitting has revealed that crystallinity and particle size mainly contributed to the increase in the photocatalytic activity.

A new clean method of hydrogen generation has been desired from viewpoints of energy and environmental issues. It is important to find various types of photocatalyst materials to see the factors affecting photocatalytic performance. Overall water splitting by semiconductor photocatalysts has attracted attention as one of the candidates.[1,2] It has been reported that many oxides consisting of d^0 transition metal cations (Ti^{4+}, Nb^{5+}, Ta^{5+}, etc.) are active photocatalysts for water splitting into H_2 and O_2 stoichiometrically under UV light irradiation.[2] Among them, $K_3Ta_3B_2O_{12}$[3,4] with a tungsten bronze structure has been reported as a borate photocatalyst. Because the BO_3^{3-} unit is triangular, borate can have a unique crystal structure. It has also been reported that the photocatalytic properties of TiO_2 were improved by boron doping.[5] However, there are few reports of boron-containing photocatalysts. Therefore, the development of new borate photocatalysts is interesting. On the other hand, metal oxide photocatalysts composed of p-block cations with d^{10} electronic configurations have been studied.[6] The photocatalysts consisting of indium, such as MIn_2O_4 (M = Ca and Sr), show high activities for water splitting under UV irradiation.[7,8] Indium compounds have also excellent capability as a semiconductive material. Rare-earth element-doped $InBO_3$ has been reported as a fluorescent material.[9–12] Therefore, authors have been interested in $InBO_3$, that is reported to be the host of luminescence materials.[10–12] $InBO_3$ with a calcite structure consists of InO_6 octahedral and BO_3 triangular units as shown in Figure 1.[9] The InO_6 octahedral units connect with each other by corner sharing, and link with the BO_3 triangular units. $InBO_3$ with unique structure like $K_3Ta_3B_2O_{12}$ has interested us in its photocatalytic properties. In the present study, the preparation conditions, photophysical properties, and photocatalytic water splitting reaction of $InBO_3$ were investigated.

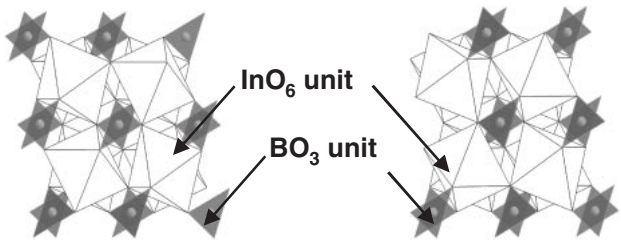

Figure 1. Crystal structure of $InBO_3$.[9]

Experimental

Indium borate powder ($InBO_3$) was prepared by a solid-state reaction[13] and a precipitation method.[14] In the case of the solid-state reaction, the starting materials, In_2O_3 (Kojundo chemical, 99.99%) and H_3BO_3 (Kanto chemical, 99.0%), were mixed well using an alumina mortar and pressed into a pellet if necessary. The mixture was calcined at 1073–1523 K for 10–72 h in air using an alumina crucible. A 10-fold excess of H_3BO_3 was added to the mixture in expectation of a flux effect. The excess boron was washed out with hot water after calcination.

$InBO_3$ was also prepared by a two-step precipitation which was an improved version of the one-step precipitation method reported by Tkachenko and co-workers.[14] In this procedure, $In(OH)_3$ and H_3BO_3 were precipitated separately. $In(NO_3)_3$ and a 5–20-fold excess of H_3BO_3 starting materials were first dissolved in hot water. An aqueous ammonia solution (Kanto chemical, conc.: 28–30%) was then added into the mixture until pH became 7 to precipitate In^{3+} to $In(OH)_3$. The solution containing the precipitate was cooled with ice, resulting in recrystallization of H_3BO_3 by temperature difference. After centrifugal separation, the precipitate mixture was dried at 333 K for 1 day in air. The obtained precursor of the mixed

Published on the web September 25, 2010; doi:10.1246/bcsj.20100137

precipitates was calcined at 823–1273 K for 0.5–10 h in air using an alumina crucible. The excess boron was washed out with hot water after the calcination.

A NiO cocatalyst was loaded by impregnation from an aqueous $Ni(NO_3)_2$ solution (Wako pure chemical, 98.0%).[15,16] The catalyst powder and the desired amount of the aqueous $Ni(NO_3)_2$ solution were put into a porcelain crucible. Water was evaporated on a water bath. The dried powder was calcined at 573 K for 1 h in air. Pretreatment by reduction with 200 Torr of H_2 at 773 K for 2 h followed by oxidation with 100 Torr of O_2 at 473 K for 1 h was carried out for the NiO-loaded photocatalyst, if necessary. A RuO_2 cocatalyst was loaded by impregnation from a carbonyl complex, $Ru_3(CO)_{12}$ (Aldrich, 99.0%), in acetone solution.[17] Acetone was evaporated on a heater. The dried powder was calcined at 673 K for 1 h in air. Ni,[18] Ru,[19,20] Pd,[19,20] and Au[21,22] cocatalysts were loaded by photodeposition from aqueous solutions of $Ni(NO_3)_2$, $RuCl_3$ (Wako pure chemical), $PdCl_2$ (Wako pure chemical, 99.9%), and $HAuCl_4$ (Wako pure chemical, 99.0%), respectively. An IrO_2 cocatalyst was loaded by oxidative photodeposition from an aqueous $(NH_4)_2IrCl_6$ solution (Wako pure chemical) in the presence of $NaNO_3$ (Kanto chemical, 99.0%) as an oxidizing reagent.[23]

The obtained powder was confirmed by X-ray diffraction using Cu Kα radiation (Rigaku, MiniFlex). Then, the amorphous component was confirmed by Raman spectroscopy (Jasco, NRS-3200). Commercially available reagents, B_2O_3 (Wako pure chemical, 90.0%) and H_3BO_3, were measured as the reference samples. The obtained catalysts were treated by hot concentrated nitric acid. Then, the obtained solution was measured by inductively coupled plasma-atomic emission spectrometry (ICP-AES, Hitachi, P-4010) to determine the chemical formula. Surface areas were determined by BET measurement (Coulter, SA3100). Photocatalysts fixed with carbon paste on a sample holder were observed by scanning electron microscopy (Jeol, JSM-6700F). Thermogravimetric-differential thermal analyses (TG-DTA) were carried out using a thermobalance (Ulvac, TGD-9600) to examine the phase transition temperature of $InBO_3$. Diffuse reflectance spectra (DRS) were obtained using a UV–vis–NIR spectrometer (Jasco, Ubest-570) and were converted from reflection to absorbance by the Kubelka–Munk method. Photoluminescence was measured in vacuum using a fluorospectrometer (Horiba, Fluorolog-3).

Photocatalytic reactions were carried out in a gas-closed circulation system. 0.5–1 g of the photocatalyst powder was dispersed in 350 mL of pure water by a magnetic stirrer. The light source was a 400 W high-pressure mercury lamp (SEN, HL400EH-5) and the reaction cell was an inner irradiation cell made of quartz. The amounts of H_2 and O_2 evolved were determined using gas chromatography (Shimadzu, GC-8A, TCD, Ar carrier).

Calculation Method. The plane-wave-based density functional theory calculation (DFT) was carried out for $InBO_3$ by employing the CASTEP program.[24] The core electrons were replaced with ultrasoft core potentials, and the valence electronic configurations for In, B, and O atoms were $4d^{10}5s^25p^1$, $2s^22p^1$, and $2s^22p^4$, respectively. The kinetic energy cutoffs were taken to be 300 eV for $InBO_3$. The calculations were carried out using the primitive unit cells of $[InBO_3]_2$, which had 34 occupied orbitals. Table 1b shows the crystal parameters for this calculation.

Table 1. (a) Parameters of the Crystal Structures of $InBO_3$ (ICSD #75254)[9] and (b) Parameters of Primitive Unit Cells of $[InBO_3]_2$ for Band Calculation

(a)	System: trigonal	$a = 4.8217$ Å	$\alpha = 90.0°$	
	Space group: $R\bar{3}cH$	$b = 4.8217$ Å	$\beta = 90.0°$	
		$c = 15.438$ Å	$\gamma = 120.0°$	
	Atom	x	y	z
	In	0	0	0
	O	0.7138	0	0.25
	B	0	0	0.25
(b)	System: rhombohedral	$a = 5.850719$ Å	$\alpha = 48.668672°$	
		$b = 5.850719$ Å	$\beta = 48.668672°$	
		$c = 5.850719$ Å	$\gamma = 48.668672°$	
	Atom	x	y	z
	In	0	0	0
	O	0.9638	−0.4638	0.25
	B	0.25	0.25	0.25

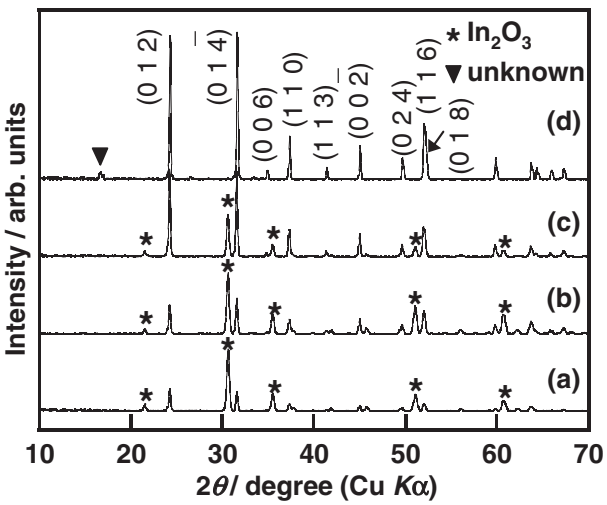

Figure 2. X-ray diffraction patterns of $InBO_3$ prepared by a solid-state reaction. Preparation conditions: (a) 1073, (b) 1173, and (c) 1273 K for 10 h, and (d) 1523 K for 72 h. A 10-fold excess of H_3BO_3 was used in the starting material.

Results and Discussion

Preparation of $InBO_3$ Particle. Figure 2 shows XRD patterns of $InBO_3$ prepared by a solid-state reaction. In_2O_3 of a starting material remained in the sample prepared by calcination at 1073, 1173, and 1273 K for 10 h even in the presence of the 10-fold amount of boric acid. The intensity of XRD patterns of $InBO_3$ to In_2O_3 increased as the calcination temperature increased. Impurities were observed in the sample prepared even at 1523 K for 72 h. It was not easy to obtain a single phase $InBO_3$ by the solid-state reaction.

Figure 3 shows XRD patterns of $InBO_3$ prepared by two-step precipitation. Tkachenko and co-workers prepared $InBO_3$

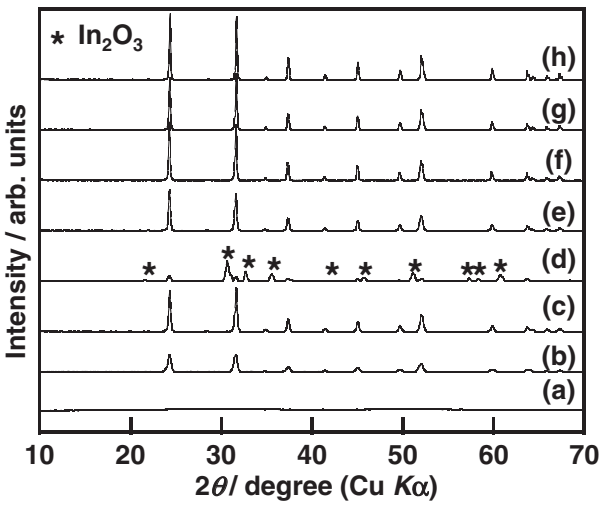

Figure 3. X-ray diffraction patterns of $InBO_3$ prepared by precipitation. Preparation conditions: (a) 823, (b) 873, (c) 973, (d) 1023, (e) 1023, (f) 1023, (g) 1073, and (h) 1273 K for 2 h. The excess amount of H_3BO_3 in the starting material: (a)–(c), (e), (g), (h) a 10-fold, (d) a 5-fold, and (f) a 20-fold.

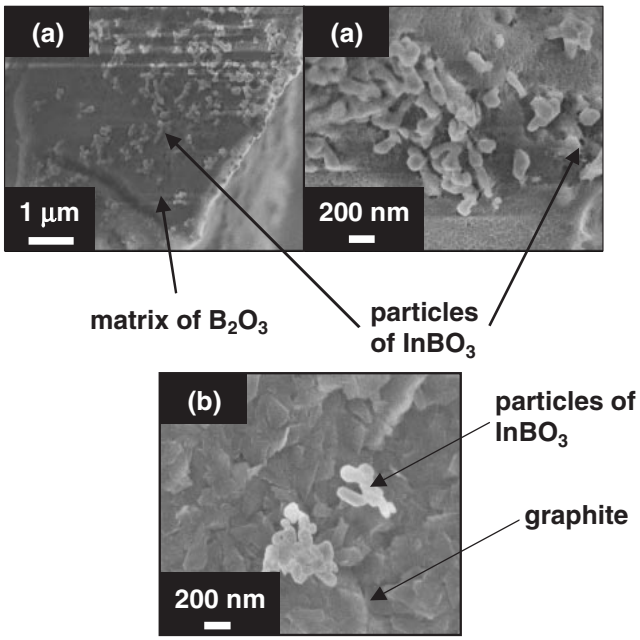

Figure 4. SEM images of $InBO_3$ prepared by precipitation. (a) Before and (b) after washing with water. Preparation conditions: 1023 K for 2 h, a 20-fold excess of H_3BO_3 was used in the starting material.

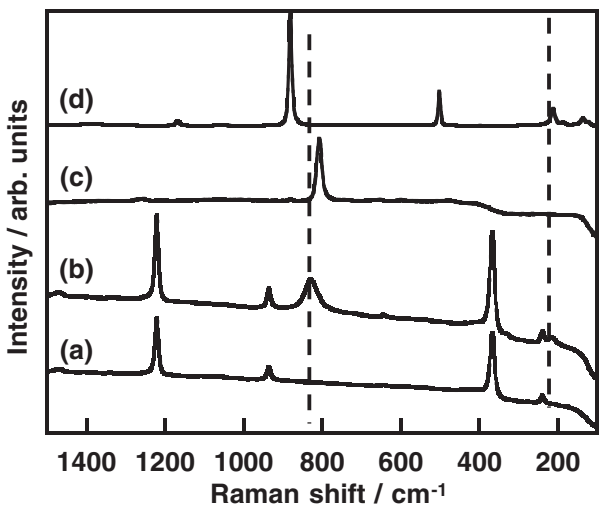

Figure 5. Raman spectra of $InBO_3$ prepared by precipitation. (a) After and (b) before washing with water, (c) B_2O_3, and (d) H_3BO_3. Preparation conditions: 1023 K for 2 h, a 10-fold excess of H_3BO_3 was used in the starting material.

in one step by precipitation using metaboric acid.[14] In contrast, we employed a two-step process using orthoboric acid. The sample obtained by calcining the precursor of the precipitation at 823 K was amorphous. Crystalline $InBO_3$ with calcite structure was obtained by calcination at 873 K for 2 h although the crystallinity was poor. This crystallizing temperature agreed with that previously reported by Tkachenko.[14] Crystallinity increased with calcination at 973 K. Thus, highly crystalline $InBO_3$ was successfully prepared by the two-step method at lower temperature and shorted calcination time than the solid-state reaction. This advantage of the two-step precipitation is thought to be as follows. Concentrations of saturated aqueous boric acid solution are 2.7% and 10% at 273 and 323 K, respectively. First, $In(NO_3)_3$ and H_3BO_3 were dissolved in water at 323 K, then the pH was adjusted to 7. It resulted in the formation of an $In(OH)_3$ precipitate.[25] The temperature of the aqueous solution containing of the $In(OH)_3$ precipitate was cooled to about 273 K resulting in the recrystallization of boric acid. Thus, the precipitate of $In(OH)_3$ was well mixed with that of boric acid, giving a good precursor. This could be the reason why the two-step precipitation gave $InBO_3$ in high quality under relatively mild preparation conditions.

The effect of excess amounts of boric acid in the preparation was examined as shown in Figure 3. A single phase of $InBO_3$ was obtained with a 10-fold excess of boric acid, but not with 5-fold. The reason why such a large amount of excess boric acid was required was not only for the compensation of loss of boric acid during recrystallization but also as a flux to enhance the crystal growth of $InBO_3$ during calcination. Samples before and after washing with hot water were measured with SEM. Small particles existed on large matrices for the sample before the wash as shown in Figure 4a, whereas the matrices disappeared resulting in only small particles remaining after the wash as shown in Figure 4b. The compositions of the small particles and the large matrices were determined by ICP-AES. The solution obtained by washing the mixture of small particles and matrices with hot water contained only boron, while indium and boron were detected in 1:1 molar ratio in a solution obtained by treatment of the small particles with nitric acid. This indicates that the small particles shown in Figure 4b were $InBO_3$. The samples before and after the washing were also measured by Raman in order to determine the large matrix as shown in Figure 5. The Raman spectrum of the sample after washing agreed with that of $InBO_3$ reported by Voron'ko,[26] indicating that the small particle was a single phase of $InBO_3$. The 644, 936, 1220, and 1470 cm^{-1} bands were assigned to the

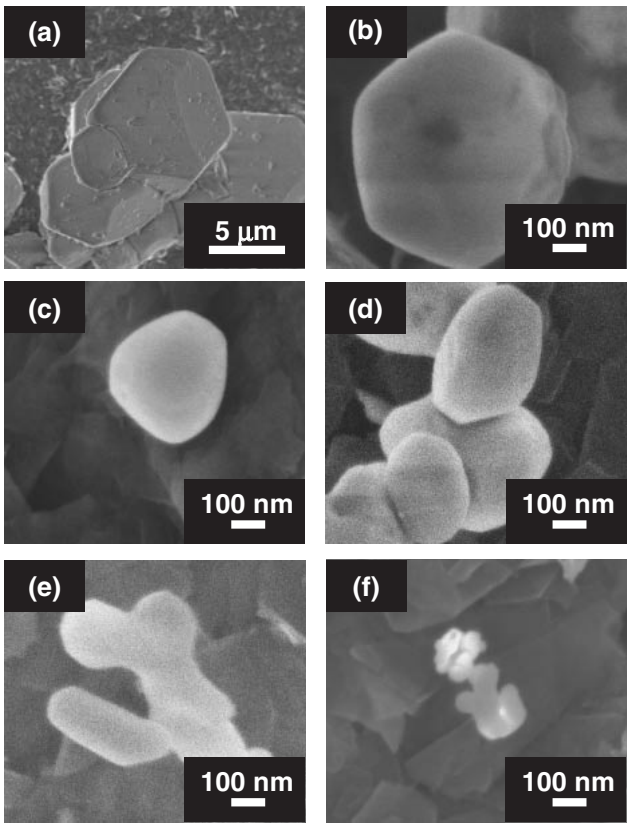

Figure 6. SEM images of $InBO_3$ prepared by (a) solid-state reaction and (b–f) precipitation. Preparation conditions: (a) 1523 K for 72 h, (b) 1273, (c) 1073, (e) 1023, and (f) 973 K for 2 h, a 10-fold excess of H_3BO_3 was used in the starting material and (d) 1023 K for 2 h, a 20-fold excess of H_3BO_3 was used in the starting material.

internal modes of the BO_3^{3-} anion, while the 237 and 365 cm^{-1} bands were assigned to external translations and librations, respectively. The ratio of the Raman band intensities of $InBO_3$ was different from that of $CaCO_3$. This difference is due to the large covalence between In^{3+} and O^{2-} of BO_3^{3-}. The samples before the washing showed peaks around 200 and 800 cm^{-1} of impurities. The peak around 200 cm^{-1} was assigned to H_3BO_3. The peak around 800 cm^{-1} positioned between those of H_3BO_3 and B_2O_3, suggesting that the large amorphous matrix was partly hydrated B_2O_3 such as metaboric acid.

Figure 6 shows SEM of $InBO_3$ prepared by a solid-state reaction and a precipitation method at different conditions. The particle size of $InBO_3$ prepared by the solid-state reaction was 5–10 μm while that prepared by precipitation was 50–200 nm. The particle size became small as the preparation temperature was lowered. Especially, 50 nm fine particles were obtained by calcination at 973 K. Next, the effect of the excess amount of boric acid on the particle size was examined. The particle size of $InBO_3$ prepared in the presence of 20-fold excess boric acid was larger than that in the presence of 10-fold. The reason why the large particle size was obtained in the presence of the large amount of excess boric acid was due to the total amount of $InBO_3$ dissolved in the borate flux. As the total amount of dissolved $InBO_3$ increased, the particle size became large during the crystal growth.

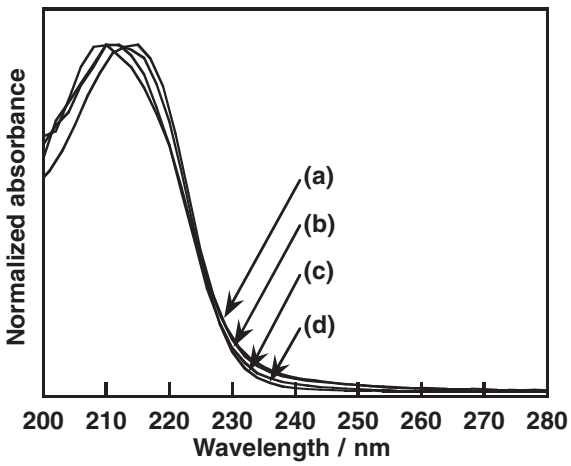

Figure 7. Diffuse reflectance spectra of $InBO_3$ prepared by precipitation. Preparation conditions: (a) 973, (b) 1023, and (c) 1273 K for 2 h, a 10-fold excess of H_3BO_3 was used in the starting material and (d) 1023 K for 2 h, a 20-fold excess of H_3BO_3 was used in the starting material.

Photophysical Properties. Figure 7 shows diffuse reflectance spectra of $InBO_3$. The onset wavelength of the absorption was 230 nm, indicating that the band gap was 5.4 eV as previously reported.[11] Figure 8 shows band structure and density of states of $InBO_3$ obtained by DFT calculation. The band structure indicated that the photoabsorption is due to indirect band gap transition. The top of the valence band was the F point (0.5, 0.5, 0.0), while the bottom of the conduction band was the Γ point. The calculated gap of the indirect transition was 3.08 eV. The direct band gap at the Γ point was 3.51 eV. The top of valence band consisted of O2p orbital. The bottom of the conduction band consisted of mainly In5s orbitals while In5p and B2s2p orbitals partially contributed to the conduction band at higher energy level. The contribution of the B2p orbitals would make the conduction band level rise, resulting in widening the band gap.

The prepared $InBO_3$ showed photoluminescence at 77 K around 450 nm as shown in Figure 9. The excitation band was observed around 230–300 nm.

Photocatalytic Water Splitting. Table 2 shows water splitting on $InBO_3$ photocatalysts under UV irradiation. Naked, Au-, Pd-, and Ru-loaded $InBO_3$ gave only small amounts of H_2 but not O_2. O_2 evolution was observed for Ni-, IrO_2-, NiO-, NiO_x-, and RuO_2-loaded $InBO_3$. Ni- and NiO-loaded $InBO_3$ produced H_2 and O_2 in 2:1 stoichiometric ratio. The NiO cocatalyst was most effective for water splitting. Thus, it was found that $InBO_3$ is a new photocatalyst for water splitting.

The effect of preparation conditions on the photocatalytic activity of $InBO_3$ was studied as shown in Table 3. The photocatalytic activity of $InBO_3$ prepared by a solid-state reaction was negligible. $InBO_3$ prepared by precipitation under different conditions was active. The activity strongly depended on the preparation temperature. The activity of $InBO_3$ prepared at 973 K was higher than that at 873 K. This was due to the increase in the crystallinity as indicated by XRD as shown in Figure 3. The decrease in the activity at high preparation temperature was due to the increase in the particle size as shown in Figure 6. This effect was also observed by the

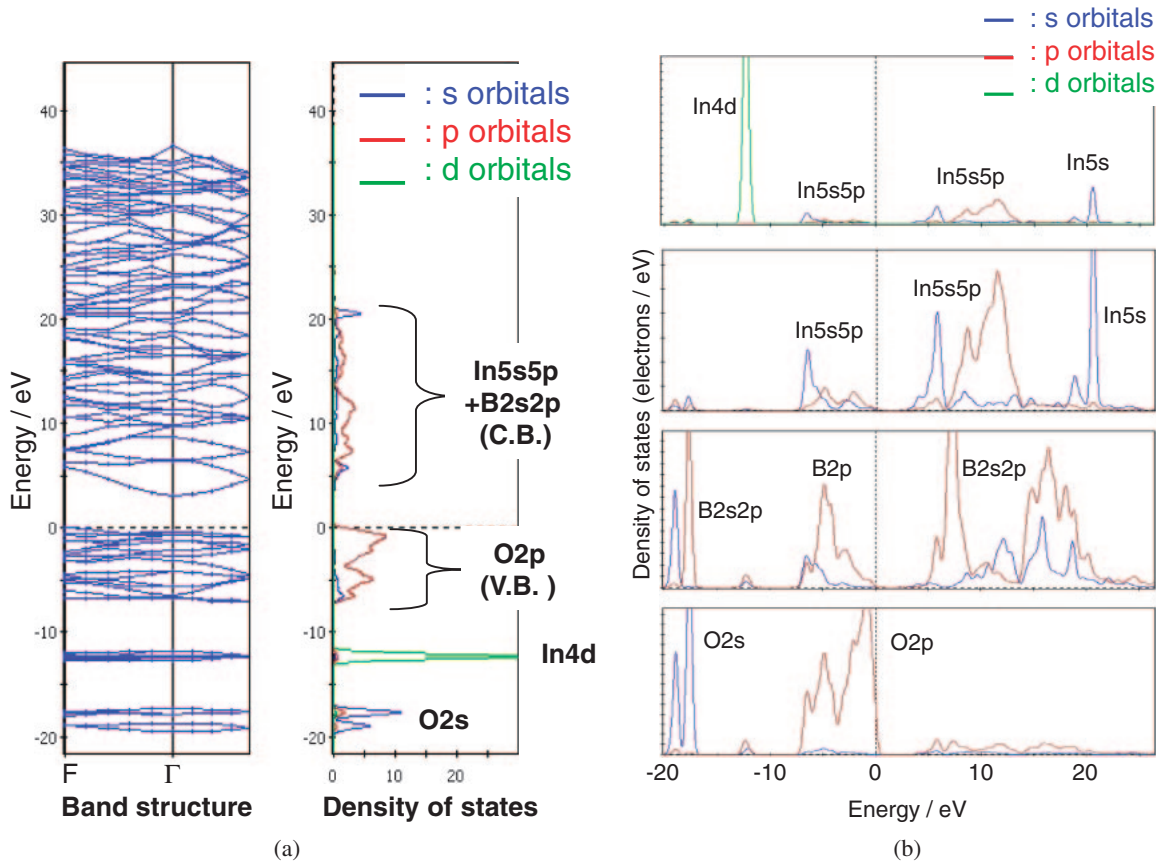

Figure 8. (a) Band structure and density of states for $InBO_3$ calculated by density functional theory and (b) partial density of states for $InBO_3$ calculated by density functional theory.

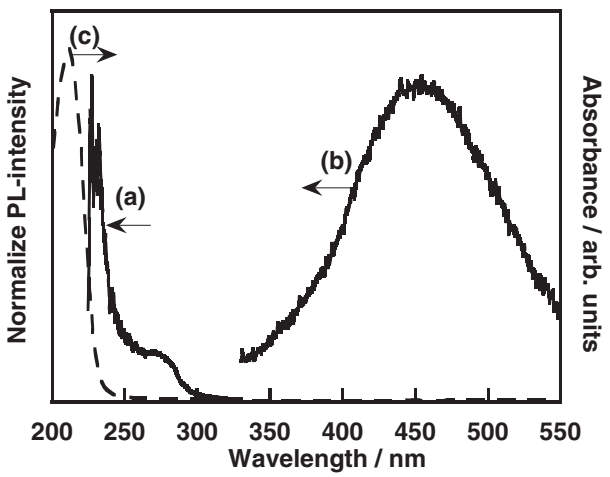

Figure 9. Photoluminescence spectra of $InBO_3$ at 77 K. (a) An excitation spectrum monitored at 430 nm and (b) an emission spectrum excited at 283 nm, and (c) a diffuse refection spectrum at room temperature.

Table 2. Effect of Cocatalysts on Water Splitting over $InBO_3$ Photocatalyst Prepared by a Precipitation Method[a)]

Cocatalyst (wt %)	Loading methods	Activity/μmol h^{-1}	
		H_2	O_2
None	—	1.3	0
Ni (1)	Photodeposition	250	127
Au (1)	Photodeposition	4.2	0
Pd (1)	Photodeposition	1.1	0
Ru (1)	Photodeposition	1.8	0
IrO_2 (1)	Photodeposition	8.0	0.5
RuO_2 (0.5)	Impregnation	8.4	0.6
NiO (0.5)	Impregnation	352	178
NiO_x (0.5)	Impregnation[b)]	20	1.3

a) Catalyst: 0.3–0.5 g, water: 350 mL, 400 W high-pressure Hg lamp, inner irradiation cell made of quartz. b) Pretreatment conditions: reduced by H_2 at 773 K for 2 h and reoxidized by O_2 at 473 K for 1 h.

comparison between $InBO_3$ photocatalysts prepared in the presence of 10- and 20-fold excess boric acid. Thus, crystallinity and particle size were important factors for photocatalytic activity of $InBO_3$ as observed for other photocatalysts.[2] Dispersion in the band structure was not good as shown in Figure 8a, suggesting that mobility of photogenerated carriers was small. In such materials, the distance that the photogenerated carriers have to migrate to the surface is important. Therefore, the activity strongly depended on the particle size as observed for the difference in the activity between $InBO_3$ prepared by solid-state reaction and precipitation. Water splitting did not proceed on the $NiO/InBO_3$ photocatalyst when a Pyrex reaction cell was employed indicating that the excitation band observed in Figures 7 and 9 was responsive to the photocatalytic reaction.

Table 3. Photocatalytic Water Splitting over NiO(0.5 wt %)/$InBO_3$

Preparation conditions		Excess amount of H_3BO_3 starting material/mol %	Molar ratio of B/In in precursor[c)]	SA /$m^2\,g^{-1}$	Particle size /μm	Activity/μmol h^{-1}	
						H_2	O_2
Solid-state reaction	1523 K for 72 h	10	—	3	1–10	3.6[a)]	0.5[a)]
Precipitation method	873 K for 2 h	10	6	15	0.05	46[b)]	8.0[b)]
	973 K for 3 h	10	6	14	0.05–0.1	398[b)]	202[b)]
	973 K for 2 h	10	6	14	0.05–0.1	352[b)]	178[b)]
	1023 K for 2 h	10	6	10	0.1–0.2	319[b)]	166[b)]
	1023 K for 2 h	20	10	6	0.1–0.2	146[b)]	70[b)]
	1073 K for 2 h	10	6	5	0.1–0.5	139[b)]	67[b)]
	1273 K for 2 h	10	6	1	0.1–1	38[b)]	17[b)]

Catalyst: a) 1 g, b) 0.5 g; water: 350 mL, 400 W high-pressure Hg lamp, inner irradiation cell made of quartz. c) Determined by ICP-AES.

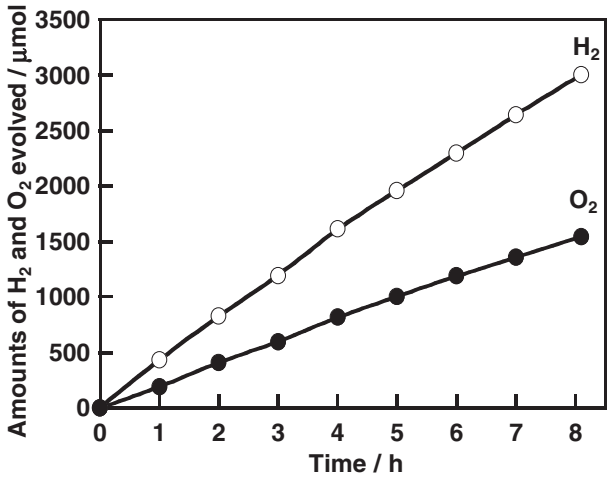

Figure 10. Photocatalytic water splitting over NiO(0.5 wt %)/$InBO_3$ prepared by precipitation and calcination at 973 K for 3 h.

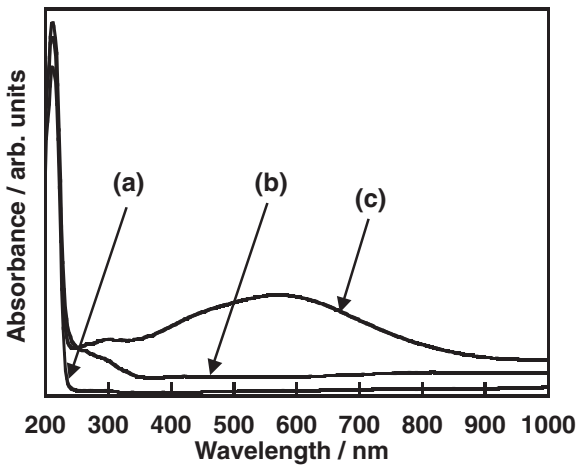

Figure 11. Diffuse reflectance spectra of (a) $InBO_3$ and NiO(1 wt %)/$InBO_3$ (b) before and (c) after photocatalytic water splitting for 8 h.

Figure 10 shows photocatalytic water splitting on NiO/$InBO_3$ prepared by precipitation at 973 K for 3 h. The color of NiO/$InBO_3$ changed from gray to deep purple during the photocatalytic water splitting. Bulky NiO cocatalyst was loaded on $InBO_3$ as usual, after impregnation. The bulky NiO probably changed into cluster-like or highly dispersed ultrafine NiO particles without long-range ordering during photocatalytic water splitting through dissolving and photodeposition of nickel species. It resulted in the color change of the NiO cocatalyst. This color after the activation was similar to that of a highly active NiO/$NaTaO_3$:La photocatalyst.[27] Figure 11 shows diffuse reflectance spectra before and after the water splitting. An absorption band around 340 nm observed before water splitting was due to the band gap transition of a NiO cocatalyst.[28] A broad absorption band around 600 nm was observed after the reaction, indicating the condition of the NiO cocatalyst changed. This color change was not observed for NiO/$InBO_3$ prepared by solid-state reaction. The activation of the NiO cocatalyst for NiO/$InBO_3$ prepared by precipitation could also contribute to high activity for water splitting.

Conclusion

Highly crystalline and fine $InBO_3$ particles were readily prepared by a two-step precipitation method compared with a solid-state reaction. The NiO-loaded $InBO_3$ powder has arisen as a new photocatalyst for water splitting. This is a novel borate photocatalyst with a calcite structure. Preparation temperature and the excess amount of boric acid in the starting material affected the crystallinity and particle size, resulting in the improvement of the photocatalytic activity.

References

1 A. Fujishima, K. Honda, *Nature* **1972**, *238*, 37.
2 A. Kudo, Y. Miseki, *Chem. Soc. Rev.* **2009**, *38*, 253.
3 T. Kurihara, H. Okutomi, Y. Miseki, H. Kato, A. Kudo, *Chem. Lett.* **2006**, *35*, 274.
4 T. Ikeda, S. Fujiyoshi, H. Kato, A. Kudo, H. Onishi, *J. Phys. Chem. B* **2006**, *110*, 7883.
5 S.-C. Moon, H. Mametsuka, E. Suzuki, M. Anpo, *Chem. Lett.* **1998**, 117.
6 Y. Inoue, *Energy Environ. Sci.* **2009**, *2*, 364.
7 J. Sato, N. Saito, H. Nishiyama, Y. Inoue, *J. Phys. Chem. B* **2001**, *105*, 6061.
8 J. Sato, N. Saito, H. Nishiyama, Y. Inoue, *Chem. Lett.* **2001**, 868.
9 J. R. Cox, D. A. Keszler, *Acta Crystallogr., Sect. C* **1994**, *50*, 1857.
10 F. J. Avella, O. J. Sovers, C. S. Wiggins, *J. Electrochem.*

Soc. **1967**, *114*, 613.
11 J. P. Chaminade, A. Garcia, M. Pouchard, C. Fouassier, B. Jacquier, D. Perret-Gallix, L. Gonzalez-Mestres, *J. Cryst. Growth* **1990**, *99*, 799.
12 T. Welker, *J. Lumin.* **1991**, *48–49*, 49.
13 T. J. Isaacs, *Experientia* **1971**, *27*, 241.
14 E. A. Tkachenko, P. P. Fedorov, S. V. Kuznetsov, V. V. Voronov, S. V. Lavrishchev, V. E. Shukshin, *Russ. J. Inorg. Chem.* **2005**, *50*, 681.
15 K. Domen, S. Naito, M. Soma, T. Onishi, K. Tamaru, *J. Chem. Soc., Chem. Commun.* **1980**, 543.
16 K. Domen, A. Kudo, T. Onishi, *J. Catal.* **1986**, *102*, 92.
17 Y. Inoue, O. Hayashi, K. Sato, *J. Chem. Soc., Faraday Trans.* **1990**, *86*, 2277.
18 K. Sayama, H. Arakawa, K. Domen, *Catal. Today* **1996**, *28*, 175.
19 J. M. Lehn, J. P. Sauvage, R. Ziessel, *Nouv. J. Chim.* **1980**, *4*, 623.
20 J. M. Lehn, J. P. Sauvage, R. Ziessel, L. Hilaire, *Isr. J. Chem.* **1982**, *22*, 168.
21 G. R. Bamwenda, S. Tsubota, T. Nakamura, M. Haruta, *J. Photochem. Photobiol., A* **1995**, *89*, 177.
22 A. Iwase, H. Kato, A. Kudo, *Catal. Lett.* **2006**, *108*, 7.
23 A. Iwase, H. Kato, A. Kudo, *Chem. Lett.* **2005**, *34*, 946.
24 M. C. Payne, M. P. Teter, D. C. Allan, T. A. Arias, J. D. Joannopoulos, *Rev. Mod. Phys.* **1992**, *64*, 1045.
25 M. Pourbaix, in *Atlas of Electrochemical Equilibria in Aqueous Solutions*, ed. by NACE International Cebelcor, Houston, Texas, **1974**.
26 Yu. K. Voron'ko, B. F. Dzhurinskii, A. E. Kokh, A. A. Sobol, V. E. Shukshin, *Inorg. Mater.* **2005**, *41*, 984.
27 H. Kato, K. Asakura, A. Kudo, *J. Am. Chem. Soc.* **2003**, *125*, 3082.
28 M. P. Dare-Edwards, J. B. Goodenough, A. Hamnett, N. D. Nicholson, *J. Chem. Soc., Faraday Trans. 2* **1981**, *77*, 643.